

## SUPPORTING INFORMATION

### **A comprehensive approach to investigate the structural and surface properties of activated carbons and related Pd-based catalysts**

A. Lazzarini,<sup>a</sup> A. Piovano,<sup>b,\*</sup> R. Pellegrini,<sup>c</sup> G. Leofanti,<sup>d</sup> G. Agostini,<sup>e</sup> S. Rudić,<sup>f</sup> M. R. Chierotti,<sup>a</sup> R. Gobetto,<sup>a</sup> A. Battiato,<sup>g</sup> G. Spoto,<sup>a</sup> A. Zecchina,<sup>a</sup> C. Lamberti<sup>a,h</sup> and E. Groppo<sup>a,\*</sup>

## S1. Chemical composition of $C_W$ and $C_{\text{Chemi}}$

Table S1. Average chemical composition (in wt%) of  $C_W$  and  $C_{\text{Chemi}}$  as determined by EDX analysis, and surface composition as determined by XPS.

Element	CW		Chemi	
	EDX (wt%)	XPS (at%)	EDX (wt%)	XPS (at%)
C	93.26	93.7	93.02	76.3
N	0.00		0.00	
O	6.33	6.3	5.73	11.9
Na	0.03		0.08	
Al	0.06		0.01	
Si	0.17	-	0.15	11.8
P	0.01		0.81	
S	0.06		0.03	
Cl	0.08		0.16	

## S2. Analysis of the XPS spectra of $C_W$ and $C_{\text{Chemical}}$

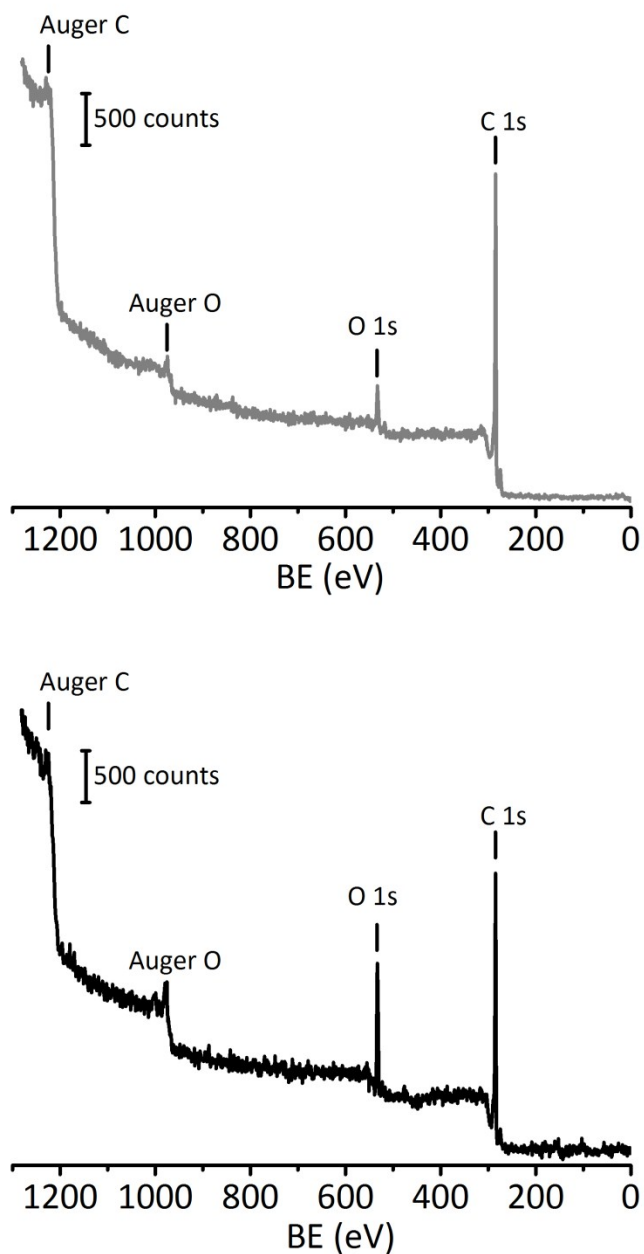


Figure S1. XPS spectra of  $C_W$  (grey) and  $C_{\text{Chemical}}$  (black) and assignment of the main bands.

Both carbons contain a substantial amount of oxygen, which is at least in part contained in inorganic ashes. Si is detected by XPS in  $C_{\text{Chemical}}$  and hardly visible in  $C_W$ .

Table S2. Results of deconvolution for XPS spectra of C<sub>w</sub>.

Peak name	EB (eV)	Area (cps eV)	Sens. Fact.	Norm. Area	Quant. At.%	Assignment	
C 1s	Peak F	290.45	17.763	97.57	5.5	93.7	$\pi$ - $\pi$ *
	Peak E	289.11	17.768	60.17	3.4		COOH + -C(O)-O-C
	Peak D	287.65	17.768	97.39	5.5	C=O, quinone	
	Peak C	286.31	17.765	165.17	9.3	C-OH + C-O-C	
	Peak B	284.47	20472.76	17.763	1152.55	65.0	Graphitic (sp <sup>2</sup> )
	Peak A	283.18	1569.71	17.760	88.38	5.0	Carbide
O 1s	532.93	5776.39	51.796	111.52	6.3	6.3	

Table S3. Results of deconvolution for XPS spectra of C<sub>chemi</sub>.

Peak name	EB (eV)	Area (cps eV)	Sens. Fact.	Norm. Area	Quant. At.%	Assignment	
C 1s	Peak F	291.81	17.754	18.24	1.9	76.3	$\pi$ - $\pi$ *
	Peak E	289.66	17.762	59.69	6.3		COOH + -C(O)-O-C
	Peak D	287.73	17.759	49.11	5.2	C=O, quinone	
	Peak C	286.21	17.765	107.94	11.3	C-OH + C-O-C	
	Peak B	284.67	7555.13	17.754	425.54	44.6	Graphitic (sp <sup>2</sup> )
	Peak A	283.75	1187.56	17.76	66.87	7.0	Carbide
O 1s	533.13	5894.65	51.796	113.80	11.9	11.9	
Si 2p	103.25	1638.30	14.56	112.52	11.8	11.8	

Table S4. Comparison of C 1s peak areas normalized to the area of peak B arbitrarily set to 100.

Sample	C 1s peak name					
	A	B	C	D	E	F
C <sub>w</sub>	7.7	100	14.3	8.4	5.2	8.5
C <sub>chemi</sub>	15.7	100	25.4	11.5	14.0	4.3

### S3. Additional SSNMR data

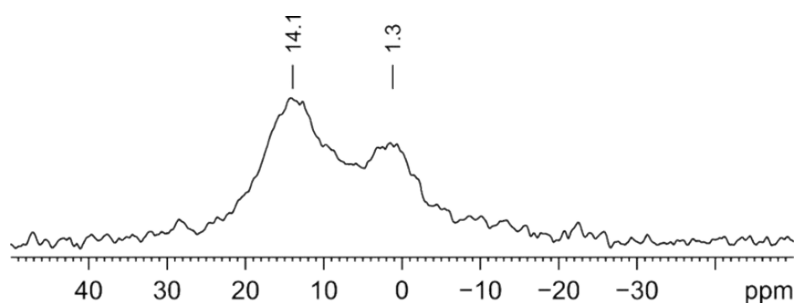


Figure S2.  $^{31}\text{P}$  (162.02 MHz) CPMAS NMR spectrum with chemical shifts for  $\text{C}_{\text{chemi}}$  recorded at 12 kHz.

The  $^{31}\text{P}$  CPMAS NMR spectrum is characterized by two main signals, centred around 1.3 and 14.1 ppm. The former is characteristic of phosphates, i.e. phosphorus bound to four oxygen atoms, likely contained in the inorganic ashes. On the contrary, the resonance at 14.1 ppm is attributed to phosphonates, i.e. organo-phosphorous compounds containing one P-C bond, revealing that at least a fraction of phosphorous has functionalized the carbon.<sup>20-23</sup>

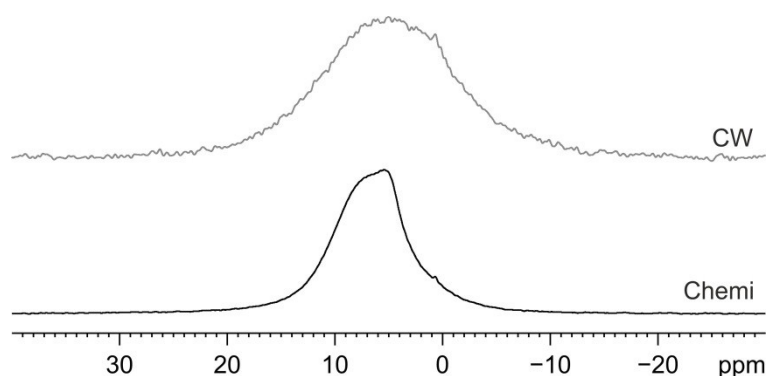


Figure S3.  $^1\text{H}$  CPMAS NMR spectra of CW and Chemi recorded at 32 kHz.

The  $^1\text{H}$  MAS NMR spectra of the two carbons show a trend similar to the  $^{13}\text{C}$  CPMAS NMR spectra. They are characterized by a single broad resonance around 5.5 ppm, with that of  $\text{C}_{\text{W}}$  (FWHM 5600 Hz) broader than that of  $\text{C}_{\text{chemi}}$  (FWHM 2850 Hz).

## S4. Additional Raman data

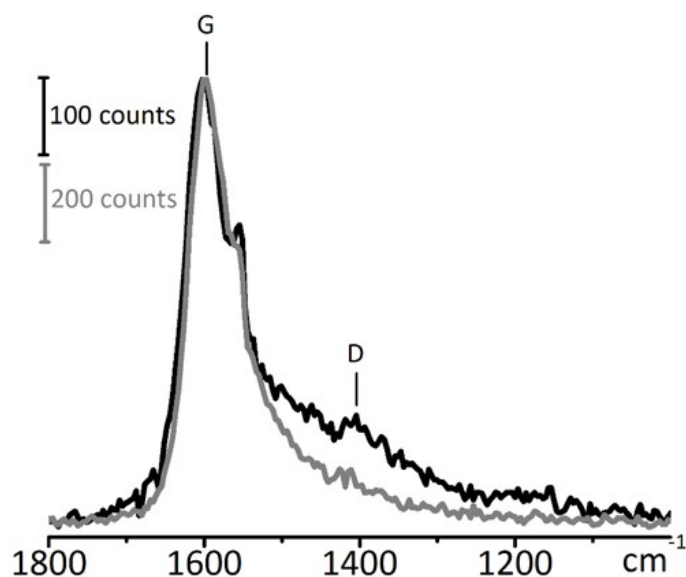


Figure S4. Raman spectra of  $\text{C}_w$  (grey) and  $\text{C}_{\text{Chemical}}$  (black) carbons (counts as a function of the Raman shift in  $\text{cm}^{-1}$ ), collected with an excitation  $\lambda$  of 244 nm, and assignment of the main bands.

Having a higher photon energy (5.1 eV), UV Raman spectroscopy excites both the  $\pi$  and the  $\sigma$  states and hence it is able to probe both the  $\text{sp}^2$  and  $\text{sp}^3$  carbon species.<sup>50</sup> Both spectra are dominated by the G band centred around 1600  $\text{cm}^{-1}$ . Opposite to what was observed in the spectra collected with the excitation  $\lambda$  of 514 nm, the spectrum of  $\text{C}_w$  is more intense than that of  $\text{C}_{\text{Chemical}}$ . In the spectrum of  $\text{C}_w$  the D band is almost absent, as expected for  $\text{sp}^2$  carbon species belonging to the islands having a graphitic order. On the contrary, a weak D band is observed in the spectrum of  $\text{C}_{\text{Chemical}}$  (around 1400  $\text{cm}^{-1}$ ). The persistence of a residual D peak is indicative of  $\text{sp}^2$  carbon species belonging to irregular  $\text{sp}^2$  domains.

## S5. Effect of graphitization on the Raman, DRIFT and INS spectra of $C_{\text{Chem}}i$

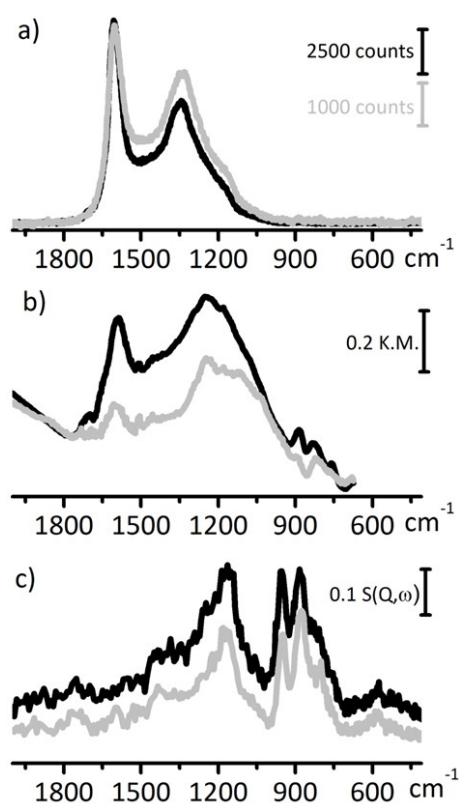


Figure S5. Raman ( $\lambda = 514$  nm, part a), DRIFT (part b) and INS (part c) spectra of  $C_{\text{Chem}}i$  measured as such (black) and heated in  $N_2$  flow at 750 °C for 2 hours (grey).

In the Raman spectrum of  $C_{\text{Chem}}i$  treated at 750 °C, the  $I(D)/I(G)$  ratio increases with respect to the spectrum of untreated  $C_{\text{Chem}}i$ , indicating that graphitization causes an ordering of the  $sp^2$  domains. In addition, the weak band around 1700  $cm^{-1}$  in the Raman spectrum of  $C_{\text{Chem}}i$ , assigned to C=O functional groups, is no more observed after the thermal treatment. The same phenomenon is even more evident in the DRIFT spectra, where the well resolved band at 1707  $cm^{-1}$  in the spectrum of  $C_{\text{Chem}}i$  totally disappears in the spectrum of the same sample treated at high temperature. Hence, graphitization occurs at the expenses of the oxygen-containing functional groups. Concerning the CH terminations, the bands associated to C-H out-of-plane vibrations decrease in intensity in both DRIFT and INS spectra of  $C_{\text{Chem}}i$  treated at 750 °C. In the DRIFT spectrum, only the band at 880  $cm^{-1}$  (*solo* species) remains well visible, whereas those at lower frequency (*duo* and *trio* species) become much less defined. In the INS spectrum, the band at 956  $cm^{-1}$  (*duo*, *trio* and *quatro* species at defective borders) is the most affected by the thermal treatment. Both observations provide an evidence that during the graphitization processes the relative fraction of irregular borders at the  $sp^2$  domains decreases in favour of the regular ones. This is reasonable because the high surface energy contained in defects of  $sp^2$  structure, such as borders and functional groups, facilitate the graphitization process.